Available online at www.sciencerepository.org

Science Repository

Research Article

Horizontal Correction of Scoliotic Deformity with High-Density Pedicle Screw Constructs: A Retrospective Analysis of 40 Patients

***Charlotte Debaud*[1,2*], *Adrien Felter*[3], *Georges Hayek*[4] *and Christian Garreau de Loubresse*[1]**

[1]*Department of Spine Surgery, HEGP University Hospital, Paris, France*
[2]*Department of Spine Surgery, Princess Alexandra Hospital, University of Queensland, Queensland, Brisbane, Australia*
[3]*Department of Diagnostic Imaging, Raymond Poincaré University Hospital, Garches, France*
[4]*Department of Diagnostic Imaging, HEGP University Hospital, Paris, France*

ARTICLE INFO

Article history:
Received: 17 October, 2020
Accepted: 29 October, 2020
Published: 10 November, 2020

Keywords:
Scoliosis surgery techniques
high-density pedicle screw constructs
de-rotation
horizontal plane
EOS imaging

ABSTRACT

Purpose: To report radiologic outcomes in the horizontal plane after scoliosis correction with high-density pedicle screw constructs through a sterEOS®-3D analysis.

Methods: We conducted a retrospective monocentric study on scoliotic patients who underwent a surgical correction with high-density constructs. SterEOS®-3D reconstructions were modelled from pre and postoperative EOS® acquisitions. Amplitude of surgical correction and residual deformity were analysed for rotational parameters (vertebrae vectors coordinates, apical vertebral rotation (AVR), intervertebral rotations, Torsion Index) and transversal offset parameters (Spread of Coronal Offsets (SCO), mean of coronal offsets (CO), T9 and L3 to Gravity Line (GL) CO, T9/L3 Transverse Gravitational Deviation Index (TGDI), T9/L3 TGDI θ categories).

Results: 80 sterEOS®3D reconstructions were analysed. Paired t-test comparisons between pre and postoperative values showed a significant reduction for Cobb angles ($p<0.0001$) and AVR ($p = 0.0024$) but not for TI ($p = 0.69$). 51% of the curves with a preoperative AVR > 10° were corrected at a segmental level with an average de-rotation amplitude of 19.3° +/- 8° and 56% at a global level with an average de-torsion index of 54% +/- 30%. Correction of SCO was effective for 95% of patients with a mean amplitude of 30mm +/- 10mm and was associated with a significant reduction in T9 and L3 to GL CO (34mm ± 24mm and 7.6mm +/-10mm respectively).

Conclusion: Horizontal corrections achieved with high-density constructs in scoliosis surgery are more significant on translation than rotation at a segmental and global level.

Introduction

The EOS® imaging system is commonly used in clinical practice to evaluate the characteristics of scoliosis, and to follow up patients after surgery while limiting the exposure to radiation [1]. The sterEOS® Spine software (EOS imaging, Paris, France) allows the 3D modelling of the entire spinopelvic complex in a standing position, giving access to an exhaustive list of angular measurements that have been shown to be accurate and reliable [2-5]. It also gives a graphic representation of the axial position and orientation of each vertebra in relation to the patient's pelvis. Although the evaluation of spine deformities in this horizontal plane has been a topic of growing clinical interest, the practical use of this sterEOS® Spine software option remains limited and the correction obtained after surgery on segmental, global rotations and on vertebral translations are still poorly understood [6, 7].

[*]*Correspondence to: Dr. Charlotte Debaud, M.D., Service de Chirurgie Orthopédique, Department of Spine Surgery, Hôpital Européen Georges Pompidou (HEGP), 20 rue Leblanc, 75015 Paris, France; Tel: +61491109062; E-mail: charlotte.debaud@hotmail.fr*

http://dx.doi.org/10.31487/j.SCR.2020.11.07

The increasing diversity of techniques in spine deformity surgery, supported by various options in terms of correction manoeuvres and hardware selection, brings further uncertainty as to what morphologic outcome is really achieved in the horizontal plane. This typically applies to high-density pedicle screw constructs which are believed to allow for good control of detorsion in addition to sagittal balance restoration through multiple vertebral anchorage points, despite the lack of strong published evidence regarding their specific effect. By reporting on pre and postoperative sterEOS® measurements in our cohort of patients, we aim to document and enhance overall thinking on techniques and objectives in spine deformity surgery. To the best of our knowledge, this study is the first to describe and quantify the amplitudes of segmental and global horizontal correction obtained with high-density pedicle screw constructs in scoliotic patients.

Materials and Methods

I Patients and Surgical Procedure

Pre and postoperative EOS® acquisitions from all scoliotic patients who underwent surgical correction and posterior vertebral fusion over a 3-year period in our department were retrospectively reviewed. Information about the use of clinical data for research studies and possible publication of findings in the academic field was provided to patients during the preoperative assessment and written signed consent was obtained for all analysed charts. Patients with a secondary scoliosis, revision surgeries, procedures including Pedicle Subtraction Osteotomy and incomplete EOS® evaluation were excluded from this study. The operator, the surgical technique and metal density were similar for all cases. Correction manoeuvres of the deformity combined segmental rod de-rotation and translation, direct vertebral de-rotation and *in situ* bending.

II SterEOS3D® Reconstruction Process and Postoperative Validity Assessment

Selected acquisitions were reconstructed by an independent spine surgeon, fully trained in the sterEOS3D® software, using the Spine module and conducting segmental adjustments on all vertebrae from T1 to L5. Upper end, apical and lower end vertebrae for each curve were manually identified on the coronal 2D view. To assess the accuracy of our reconstruction process on instrumented vertebrae, we selected 10 postoperative acquisitions from patients with a radiographic follow-up including a computed-tomography scan (CT). SterEOS3D® apical axial vertebral rotation (AVR) for each residual curve was compared with corresponding CT measurements, performed by an independent radiologist, applying the method of Ho *et al.* on overlaid slides, with the patient's pelvis as a reference. Statistical analysis was performed using both linear regression and Bland-Altman plot [8]. The limits of agreements were used as thresholds to define a non-null AVR in our main analysis.

III Radiographic Parameters

Besides Cobb angles and pelvic parameters, T1 to L5 axial vertebral rotations, intervertebral axial rotations (IAR), vertebral transversal coordinates (X; Y) and the coronal offsets (CO) of T9/L3 (X_{T9} / X_{L3}) were also measured. In the vertebra vector basis, we chose to approximate the theoretical position of the line of gravity (GL) by the Central Hip Vertical Axis (CHVA) (Figure 1) [9, 10]. Out of this raw data the following horizontal parameters were calculated :

Torsion Index $TI = \left(\left|\sum \mathrm{IAR}_{\mathrm{upper\ part}}\right| + \left|\sum \mathrm{IAR}_{\mathrm{lower\ part}}\right|\right)$

Spread of Coronal Offset $SCO = X_{max} - X_{min}$

$Mean\ of\ CO = \sum |Xv| \div number\ of\ vertebrae$

T9 and L3 Transverse Gravitational Deviation Indexes

$T9/L3\ TGDI\ offset = \sqrt{\left({X_{T9/L3}}^2 + {Y_{T9/L3}}^2\right)}$

$T9/L3\ TGDI\ \theta = \cos^{-1}\left[X_{T9/L3} \div \sqrt{\left({X_{T9/L3}}^2 + {Y_{T9/L3}}^2\right)}\right]$ [7, 11].

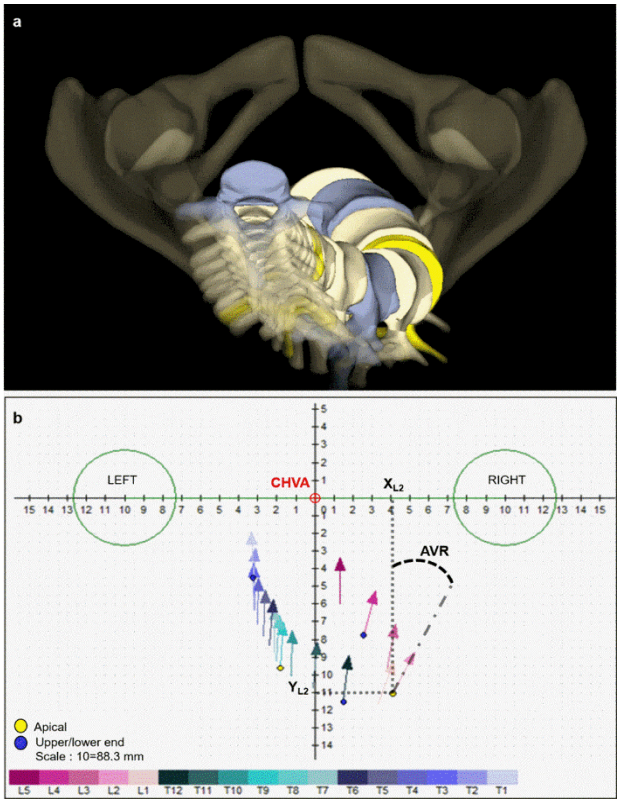

Figure 1: EOS graphic representations in the horizontal plane. **a)** Full sterEOS3D Spine reconstruction in top view. **b)** Corresponding vectorial chart. Patient's basis is centred on the Central Vertical Hip Axis (CHVA), each vertebra is represented by its axial vector. The convention of sign for the apical vertebra's axial rotation (AVR) in this basis is clockwise/negative and counterclockwise/positive. The coordinates (Xv; Yv) of the vertebral vector's origin define the location of each vertebra within the patient's basis.

IV Correction Analysis

We first estimated the surgical correction of Cobb angles, axial rotations and horizontal translations by comparing pre and postoperative values. We further analysed the de-rotation effect of surgery at the segmental level by evaluating the amplitudes of correction (or worsening) and the residual AVR values of AVR, and globally by calculating detorsion indexes $DI = 100 \times \left(TI_{preop} - TI_{postop}\right) \div TI_{preop}$ [12]. Offsets correction was determined based on the amplitudes of translation. We

used T9 and L3 TGDI categories to describe the effect of surgeries on combined coronal and sagittal malalignment [7].

V Statistical Analysis

Patient characteristics are presented as mean values with standard deviation (±SD) unless specified otherwise. Wilcoxon matched pairs signed rank test was used to compare pre and postoperative non-parametric variables. Mann-Whitney test was used to compare preoperative means between AIS and ADS groups. Fischer's exact test was used to assess contingency between AVR and TI corrections. Statistical analysis was done using GraphPad Prism version 8.0 (GraphPad Software, La Jolla California USA).

Results

I Assessment of sterEOS® Validity for Postoperative Rotation Measurement

Patients selected for the preliminary assessment of postoperative AVR sterEOS® measurements' accuracy all had symptomatic Adult Degenerative Scoliosis (ADS, n=10).

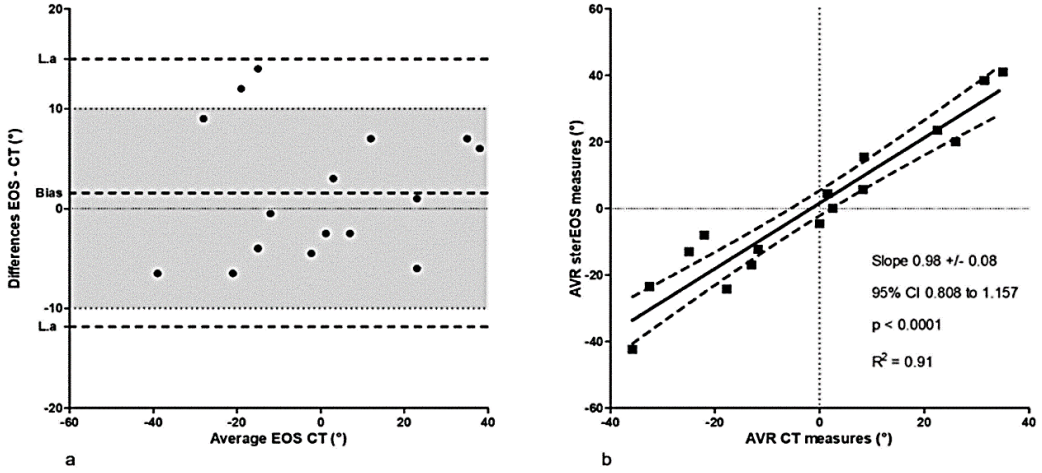

Figure 2: SterEOS®-3D accuracy for postoperative AVR. **a)** Bland-Altman plot illustrating the concordance in AVR measurements from sterEOS® and CT scans. Bias = 1,563; SD of bias 6,8; 95% Limits of agreement (L.a) -11,85 to 14,98. **b)** General linear modeling plot of the relationship between sterEOS® and CT scan-derived AVR measurements in residual curves after surgery. CI indicates the 95% confidence interval.

On the last follow-up after surgery, 16 residual curves with a Cobb angle >10° were identified. Means for absolute AVR values measured from sterEOS®3D reconstructions or CT images were very similar, 18.3° ± 13.3° versus 18.3° ± 12.1°, respectively. Consistent with this, linear regression showed a direct positive and highly significant correlation between sterEOS® and CT measurements (p<0.000) (Figure 2a). On Bland-Altman plot, the observed bias was 1.625 and the limits of agreement were -11.69 and 14.94. The difference between EOS® and CT measurement was < 10° for 14 out of 16 curves (Figure 2b).

II Study Population

Our main analysis was conducted on 80 reconstructions retrieved from our retrospective monocentric mono-operator cohort (Figure 3). Patients included in this sterEOS3D® analysis had either idiopathic (55%) or degenerative scoliosis (45%). Clinical features and characteristics of spine deformity are shown in (Table 1**)**. From the 40 preoperative sterEOS3D© reconstructions, 76 curves with a Cobb angle > 10° were identified. The average Cobb angle, absolute AVR value and TI were 41° ± 17°, 15° ± 11° and 22° ± 14°, respectively. For 56.5 % of the identified curves (43 out of 76), absolute AVR values were > 10°, with an average of 23° ± 9.5°.

Table 1: Demographics and deformity.

	Group AIS n = 22		**Group ADS n = 18**	
Age at surgery (yrs) Mean [min;max]	22 [13;36]		60 [43;73]	
Last follow-up (months) Mean [min;max]	18 [6;35]		20 [6;38]	
Gender F/M	15/7		17/18	
Number of instrumented vertebrae Mean [min;max]	10,8 [6;14]		12 [6;17]	
Curve types % of patients	**Lenke**		**SRS-Schwab**	
	1A	52	**T**	5,5
	1B	11	**L**	22
	5C	32	**D**	44,5
	6C	5	**N**	28

PT (°) Mean +/- SD	6,5 +/- 7,7	17,4 +/- 6,9
SVA (mm) Mean +/- SD	1 +/- 21,8	26,4 +/- 25,8
PI (°) Mean +/- SD	46 +/- 10,2	50,5 +/- 17,3
PI – LL mismatch (°) Mean +/- SD	-2 +/-13,6	14 +/- 13,7
Number of curves with Cobb >10°	46	38

Demographics and deformity parameters in patients with Adolescent Idiopathic Scoliosis (AIS) or Adult Degenerative Scoliosis (ASD). Curve Types referred to Lenke and SRS-Schwab coronal classifications [24, 25]. F, Female; M, Male; PT, Pelvic Tilt; SVA, Sagittal Vertical Axis; PI, Pelvic Incidence; LL, Lumbar Lordosis.

Table 2: Pre and postoperative sterEOS3D measurements of Cobb and horizontal parameters.

	Total Curves	**AIS Curves**	**ADS Curves**
Pre-operative measurements			
n	76	43	33
Cobb angle	41 ± 17	42 ± 18	38 ± 15
Rotation Index			
AVR	15 ± 11	13 ± 10	18 ± 13
TI	22 ± 14	18 ± 11	27 ± 16
Translation Index			
SCO	54 ± 18	56 ± 20	51 ± 16
Mean of CO	22 ± 11	23 ± 10	21 ± 12
T9 to GL CO	30 ± 22	38 ± 21	21 ± 21
L3 to GL CO	21 ± 13	18 ± 12	26 ± 14
T9 TGDI offset	79 ± 24	77 ± 26	83 ± 20
T9 TGDI θ category	0/0/23/0/17	0/0/17/0/5	0/0/6/0/12
L3 TGDI offset	44 ± 26	30 ± 18	62 ± 23
L3 TGDI θ category	1/3/23/0/13	1/3/14/0/4	0/0/9/0/9
Post-operative measurements			
n	73	45	34
Cobb angle	19 ± 14 *** (p<0,0001)	18 ± 14 *** (p<0,0001)	19 ± 14 *** (p<0,0001)
Rotation Index			
AVR	11 ± 10 ** (p=0,0024)	10 ± 9 * (p = 0,0353)	12 ± 12 ** (p = 0,0081)
TI	19 ± 15 *ns* *(p = 0,69)*	17 ± 15 *ns* *(p=0,8922)*	21 ± 15 *ns* *(p=0,0973)*
Translation Index			
SCO	25 ± 11 *** (p<0,0001)	24 ± 13 *** (p<0,0001)	27 ± 8 *** (p = 0,0006)
Mean of CO	13 ± 7 *** (p<0,0001)	12 ± 5 *** (p<0,0001)	15 ± 9 * (p = 0,0366)
T9 to GL CO	12 ± 9 *** (p<0,0001)	12 ± 10 *** (p = 0,0001)	12 ± 9 *ns* (*p = 0,3380)*
L3 to GL CO	14 ± 9 *** (p=0,0002)	12 ± 8 * (p=0,0251)	15 ± 9 ** (p=0,0027)
T9 TGDI offset	77 ± 17 *ns* *(p = 0,2088)*	70 ± 16 * (p=0,0477)	81 ± 23 *ns* *(p=1)*
T9 TGDI θ category	0/0/2/0/42	0/0/1/0/21	0/0/1/0/17
L3 TGDI offset	36 ± 14 *ns* *(p = 0,0627)*	24 ± 35 *ns* *(p=0,9224)*	37 ± 50 * (p=0,0210)
L3 TGDI θ category	3/1/18/0/18	3/1/8/0/10	0/0/10/0/8

Mean Values ±Standard Deviation are reported. Wilcoxon matched-pairs signed rank test was used to compare pre and postoperative values* Statistical significance p < 0,05, ns non-significant Cobb angle and Rotation index are expressed in °, Translation index in mm except forT9 and L3 TGDI θ category for which are reported the number of patients in each category I/II/III/IV/V AIS, Adolescent Idiopathic scoliosis; ADS, Adult Degenerative Scoliosis; AVR, Apical Vertebral Rotation; TI, Torsion Index; SCO, Spread of Coronal Offsets; CO, Coronal Offsets; GL, Gravity Line; TGDI, Transverse Gravitational Deviation Index.

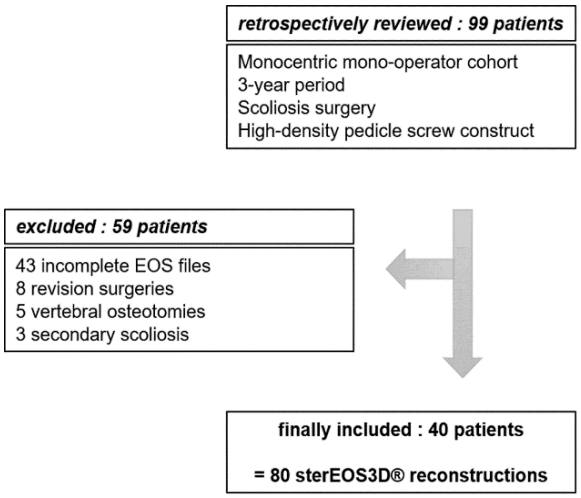

Figure 3: Flowchart of the sterEOS3D® analysis.

We retrospectively checked and confirmed that all curves associated with a significant AVR were included in the surgical construct. In terms of translation, the average SCO was 54 mm ± 18mm; 85 % of patients (n=34) were categorized either in T9, L3, or both (T9/L3 TGDI θ category III; combined sagittal and coronal malalignment). Preoperative means and standard deviations for Rotation and Translation indexes are shown in (Table 2**)**. Since our patients' cohort displayed half idiopathic and half degenerative deformities, we sought differences between the two subgroups in preoperative measurements. TI and L3 TGDI offset were significantly higher in the ASD group whereas T9 to GL coronal offset was significantly higher in the AIS group (Figure 4). All AIS patients displayed a combined sagittal and coronal malalignment [T9 TGDI θ category III (n=8) or L3 TGDI θ category III (n=5), or both T9/L3 TGDI θ category III (n=9)], versus 66% of ADS patients [(T9 TGDI θ category III: n=3; L3 TGDI θ category III: n=6; T9/L3 TGDI θ category III: n=3)]. For 33% of ADS patients, the imbalance was mainly sagittal.

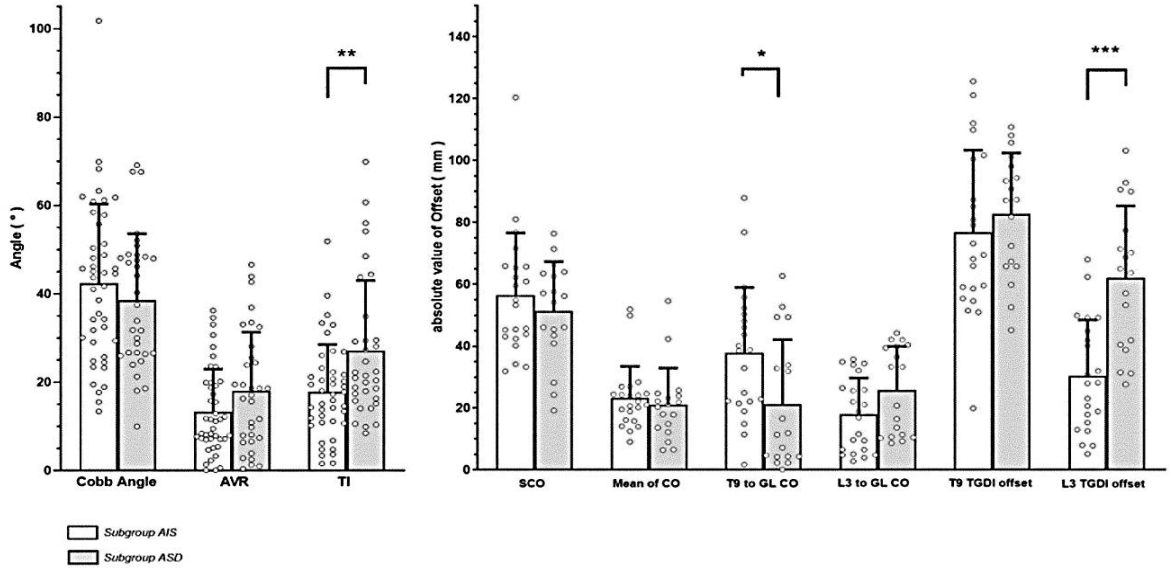

Figure 4: Preoperative sterEOS®-3D measurements in patients with adult idiopathic scoliosis (AIS) compared to those with degenerative adult spinal deformity (ASD). Each plotted dot represents a curve and bars are means +/- SD. Comparison of rotation showed a significant difference in Torsion indexes (unpaired t-test p = 0.0032); Translation index comparisons showed a significant difference in T9 to GL CO (unpaired t-test p = 0.018), and in L3 TGDI offset (unpaired t-test p < 0.0001). SCO, Spread of Coronal Offset; GL, Gravity Line; CO, Coronal Offset; TGDI, Transverse Gravitational Deviation Index.

III Surgical Corrections

Wilcoxon test comparisons between pre and postoperative values showed a significant reduction in Cobb angles (p<0.0001) and AVR (p = 0.0024) but not TI (p = 0.69). Translation indexes were all significantly reduced except T9 and L3 TGDI offset (p = 0.1683 and p = 0.0627, respectively). To better describe the results in relation to Rotation Indexes, we next examined the 43 curves associated with a preoperative AVR > 10°. This threshold was chosen according to the limits of agreements displayed in the Bland-Altman plot, thus taking into account the error linked to our stereos®3D measurement.

The surgical effect was also deemed to be significant when the differential between pre and postoperative AVR values was >10°. Specifically, 51% of the curves (22 out of 43) were effectively corrected at a segmental level and the amplitude of correction averaged 19.3° ± 8°, with a postoperative AVR ranging between -10° and 10° for 15 curves (Figure 5). The differential between pre and postoperative AVR values for the 21 non-corrected curves averaged 3.5°± 3°. At a global level (TI), 56% of the curves (24 out of 43) were corrected and for these, the de-torsion index mean was 54% ± 30%. For the 19 curves which displayed a worsened postoperative TI, the average increase of TI was 56% ±48%. Overall, there was no significant difference in the proportion of efficiently de-rotated curves between idiopathic and degenerative scoliosis groups. Besides, there was no contingency between AVR and TI corrections (Fischer's exact test, p = 0.18).

Translation analysis revealed that the average SCO correction was 29mm ± 13mm. Of all the 40 analysed reconstructions, 38 displayed a SCO reduction >10 mm, with an average of 30.6 mm ± 10.4mm. Overall,

the mean of coronal offsets along the spine was corrected by 9.5 mm ± 11mm. T9 to GL coronal offset and T9 TGDI offset were significantly corrected in the AIS group and the average correction were 34mm ± 24mm (p=0.0001) and 6.6mm ± 22mm (p=0.0477), respectively. L3 to GL coronal offset was significantly corrected in both groups with an average decrease of 7.6mm ±10mm (p=0.0002), whereas the correction of L3 TGDI offset was only significant in the ADS group (18mm ± 27mm, p=0.021). Overall, 21 out of the 23 deformities that were categorized in T9 TGDI θ category III preoperatively were corrected into category V, whereas only 11 out of 23 went from L3 TGDI category III to category I or V. For patients categorized in L3 TGDI θ category III after surgery, the correction of L3 TGDI offset was significant (p = 0.0035), and the evaluation of standard 2D parameters showed an appropriate sagittal balance, with postoperative angles / distance for lumbar lordosis, pelvic incidence, sacral slope, pelvic tilt and SVA being 53° ± 11°, 53° ± 16°, 39° ± 9°, 14° ± 10°, and 3.5mm ± 26mm, respectively (means ± SD). The radiographic case presented in (Figure 6) illustrates efficient outcomes on translation indexes despite residual postoperative global and segmental rotations.

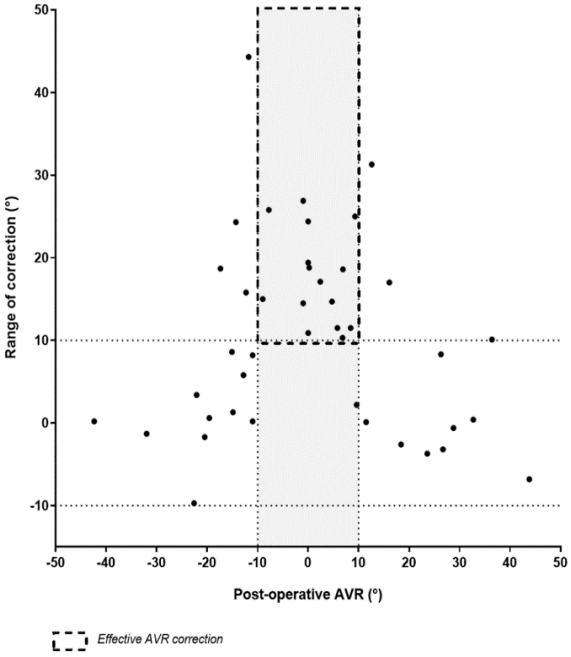

	Surgical correction	No correction
AVR reduced to [-10°;10°]	15/43 *Effective correction*	
Post-operative AVR < -10° or > +10°	7/43 *Correction with significant Residual AVR*	20/43 *No correction*

Figure 5: Effect of surgery on AVR correction. Analysis of 43 curves associated with a significant preoperative AVR (< -10° or > +10°). Scattered dots show the range of rotational correction and the final AVR for each curve. Table values are the number of curves in each correction category. A clinically adequate correction was considered to combine a significant surgical de-rotation effect > 10° with a postoperative AVR ranging between [-10°;10°].

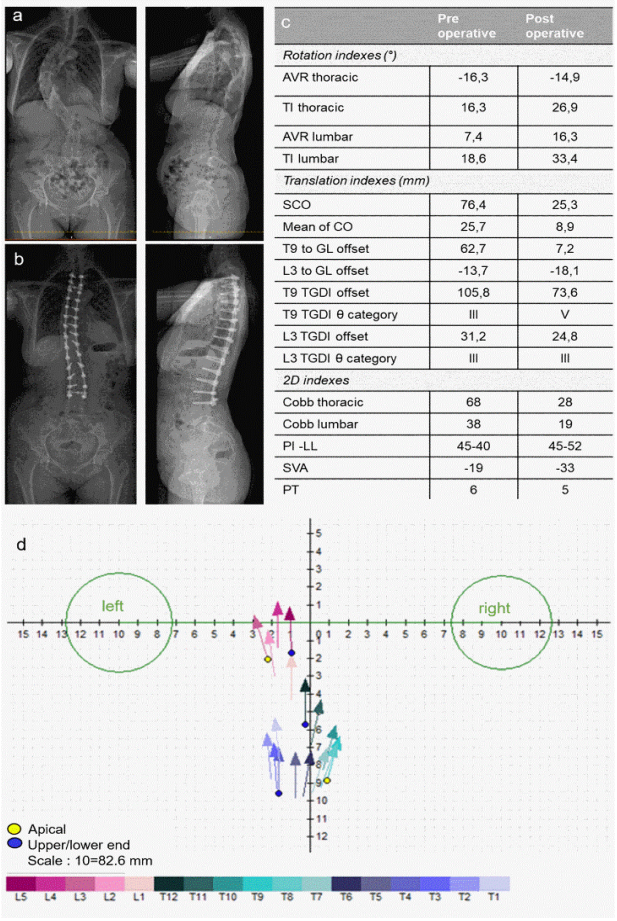

c	Pre operative	Post operative
Rotation indexes (°)		
AVR thoracic	-16,3	-14,9
TI thoracic	16,3	26,9
AVR lumbar	7,4	16,3
TI lumbar	18,6	33,4
Translation indexes (mm)		
SCO	76,4	25,3
Mean of CO	25,7	8,9
T9 to GL offset	62,7	7,2
L3 to GL offset	-13,7	-18,1
T9 TGDI offset	105,8	73,6
T9 TGDI θ category	III	V
L3 TGDI offset	31,2	24,8
L3 TGDI θ category	III	III
2D indexes		
Cobb thoracic	68	28
Cobb lumbar	38	19
PI -LL	45-40	45-52
SVA	-19	-33
PT	6	5

Figure 6: Clinical case of a 56-year-old woman who underwent a T3L4 posterior fusion instrumented with a high-density pedicle screw construct. **a) & b)** 2D EOS antero-posterior and lateral views of the spine deformity **a)** before and **b)** after surgery. **c)** Horizontal and 2D pre and postoperative parameters retrieved from the sterEOS®3D Spine software. Analysis of radiographic outcomes in the horizontal plane shows the absence of segmental de-rotation, significant residual thoracic and lumbar AVR, and the worsening of Torsion indexes. These results are, however, outweighed by an important correction of translation for the main thoracic curve. 2D indexes and decreased L3 TGDI offset confirm the restauration of an adequate sagittal balance. The residual malalignment of L3 (TGDI category III) is related to its coronal offset. **d)** Postoperative vertebra vectors chart illustrating the global realignment of vertebrae alongside the sagittal axis despite residual rotations.

Discussion

Our study investigated the amplitude of correction achieved in the horizontal plane with high-density pedicle screw constructs in spine deformity surgery, using the sterEOS®3D software to measure rotation and translation indexes in standing position before and after surgery. We found that the transverse correction was systematic and efficient for offsets but varied sharply between cases for rotations. This outcome was highlighted in both AIS and ADS patients.

To the best of our knowledge, this is the first study to report a comprehensive sterEOS®3D analysis of the radiologic outcomes

achieved on transverse parameters in scoliotic patients, taking into consideration both rotation and translation indexes.

In a preliminary step, we confirmed that the correlation between our SterEOS®3D postoperative AVR measurements and tomographic results was significant. The accuracy of SterEOS®3D measurements in the horizontal plane, especially on instrumented vertebrae remains poorly documented. Yet, the 3D reconstruction process on instrumented spines is often challenging since the presence of hardware can overshadow the antero-posterior radiologic landmarks used to perform segmental adjustments that determine the accurate modelling of vertebral rotation. The lack of published evidence to demonstrate the SterEOS®3D software accuracy in the horizontal plane may be explained by the limitations and drawbacks of comparison with the gold-standard tomographic method. Indeed, besides radiation exposure and cost, it is commonly argued that vertebral rotation may be modified when a scoliotic patient lies down in supine position. This latter factor has probably a minimal impact after surgery. Therefore, and despite a relatively low number of pairings, we relied on the limits of agreements highlighted in our preliminary comparative study to take into account the possibility of a 10° error on rotation measurements for the radiographic outcomes in our cohort.

Overall, our average pre and postoperative values of AVR and TI were consistent with published reports referring to sterEOS®3D evaluation of the rotation corrections that were achieved in scoliotic patients [10, 11, 13, 14]. Our results confirmed some of the findings previously reported by Courvoisier *et al.*, especially the absence of interdependency between global (TI) and segmental (AVR) rotation correction [13]. It seems important to underline the technical implications related to this observation. In practice, an appropriate correction strategy should take into account the fact that segmental de-rotation manoeuvres applied on the apex of the curve do not warrant its detorsion. Using means comparisons, we also confirmed that the reduction of rotational angles after surgery was significant for AVR but not for TI. However, when taking into account the direction of correction, we showed that the effect of high-density constructs on global torsion was significant in terms of amplitude but split between correction and worsening in the final outcome. An efficient detorsion of the deformity was achieved in about half of our cases. The effect on segmental rotation appeared to be more casual, split between efficient de-rotation and no change in terms of amplitude. This highlight goes against the argument that more vertebral implants allow for a better de-rotation at the apex of the curve and adds to the ongoing debate regarding the effect of anchor density on surgical correction in spine deformity [15, 16].

Many studies have compared high and low metal density constructs in AIS patients [14, 17-20]. Overall, these works focused on coronal curve and thoracic kyphosis correction, and seemingly agreed to conclude that more pedicle screws do not lead to better radiologic outcomes, but do increase cost, procedure duration and surgical risks associated with screw misplacement. Nevertheless, none of these comparisons included transverse indexes and the approximation of vertebral translation with Cobb angles has been shown to present some limitations [21]. Our analysis clearly underlines the efficiency of high-density constructs to support a steady and significant correction of offsets, regardless of de-rotation. The evaluation of T9 and L3 TGDI confirmed that this offset correction was effective in both the coronal and the sagittal planes for 91% of main thoracic curves. In cases presenting with a L3 TGDI category III malalignment after the surgery, the offset correction was nevertheless effective. This result was supported by the analysis of 2D sagittal parameters, which interestingly showed an adequate sagittal balance [12, 22, 23]. This finding is consistent with a recent publication showing of a strong correlation between L3 TGDI offset and health-related quality of life in ADS patients before surgery and thus indicates that L3 TGDI offset could replace our standard 2D sagittal analysis method in the horizontal plane following long posterior spine instrumentation [7].

Our study has several methodologic and conceptual limitations. Mainly, by being descriptive, it does not address the clinical correlation linked to the described radiographic outcomes in the horizontal plane. It is also important to point out that any effect(s) of surgical manoeuvres applied by the operator and the use of high-density anchor instrumentation could not be differentiated in our analysis. Despite these limitations, our work demonstrates how the surgical effect supported by high-density pedicle screw constructs on translation indexes could take place at the expense of global and segmental rotation correction and raises the question which clinical impact these postoperative residual rotations actually have on the functional and long-term surgical outcomes in scoliotic patients. It also underlines how a more systematic integration of horizontal parameters in biomechanical studies could help guide evidence-based clinical practice when it comes to the choice of surgical technique and instrumentation in spine deformity surgery.

Acknowledgments

We thank Gautier Debaud, senior teacher in mathematics for his assistance with formula programming in Microsoft Excel; Dr Kate Campbell and A/Prof Marc Ruitenberg for critical reading and helpful comments on the manuscript.

Conflicts of Interest

None.

Ethical Approval

Ethical approval was waived by the local Ethics Committee of University A in view of the retrospective nature of the study and all the procedures being performed were part of the routine care.

Consent

Informed consent was obtained from all individual participants included in the study.

Data Availability

All data generated or analysed during this study are included in this published article (and its supplementary information file).

REFERENCES

1. Dietrich TJ, Pfirrmann CWA, Schwab A, Pankalla K, Buck FM (2013) Comparison of radiation dose, workflow, patient comfort and financial break-even of standard digital radiography and a novel biplanar low-dose X-ray system for upright full-length lower limb and whole spine radiography. *Skeletal Radiol* 42: 959-967. [Crossref]
2. Humbert L, De Guise JA, Aubert B, Godbout B, Skalli W (2009) 3D reconstruction of the spine from biplanar X-rays using parametric models based on transversal and longitudinal inferences. *Med Eng Phys* 31: 681-687. [Crossref]
3. Somoskeöy S, Tunyogi Csapó M, Bogyó C, Illés T (2012) Accuracy and reliability of coronal and sagittal spinal curvature data based on patient-specific three-dimensional models created by the EOS 2D/3D imaging system. *Spine J* 12: 1052-1059. [Crossref]
4. Ilharreborde B, Steffen JS, Nectoux E, Vital JM, Mazda K et al. (2011) Angle measurement reproducibility using EOS three-dimensional reconstructions in adolescent idiopathic scoliosis treated by posterior instrumentation. *Spine* 36: E1306-E1313. [Crossref]
5. Rehm J, Germann T, Akbar M, Pepke W, Kauczor HU et al. (2017) 3D-modeling of the spine using EOS imaging system: Inter-reader reproducibility and reliability. *PLoS One* 12: e0171258. [Crossref]
6. Courvoisier A, Drevelle X, Dubousset J, Skalli W (2013) Transverse plane 3D analysis of mild scoliosis. *Eur Spine J* 22: 2427-2432. [Crossref]
7. Moke L, Overbergh T, Severijns P, Schelfaut S, Moens P et al. (2020) The Transverse Gravitational Deviation Index, a Novel Gravity Line-Related Spinal Parameter, Relates to Balance Control and Health-Related Quality of Life in Adults With Spinal Deformity. *Spine* 45: E25-E36. [Crossref]
8. Ho EK, Upadhyay SS, Chan FL, Hsu LC, Leong JC (1993) New methods of measuring vertebral rotation from computed tomographic scans. An intraobserver and interobserver study on girls with scoliosis. *Spine* 18: 1173-1177. [Crossref]
9. Illés T, Tunyogi Csapó M, Somoskeöy S (2011) Breakthrough in three-dimensional scoliosis diagnosis: significance of horizontal plane view and vertebra vectors. *Eur Spine J* 20: 135-143. [Crossref]
10. Illés T, Somoskeöy S (2013) Comparison of scoliosis measurements based on three-dimensional vertebra vectors and conventional two-dimensional measurements: advantages in evaluation of prognosis and surgical results. *Eur Spine J* 22: 1255-1263. [Crossref]
11. Steib JP, Dumas R, Mitton D, Skalli W (2004) Surgical correction of scoliosis by in situ contouring: a detorsion analysis. *Spine* 29: 193-199. [Crossref]
12. Kim YJ, Bridwell KH, Lenke LG, Rhim S, Cheh G (2006) An analysis of sagittal spinal alignment following long adult lumbar instrumentation and fusion to L5 or S1: can we predict ideal lumbar lordosis? *Spine* 31: 2343-2352. [Crossref]
13. Courvoisier A, Garin C, Vialle R, Kohler R (2015) The change on vertebral axial rotation after posterior instrumentation of idiopathic scoliosis. *Childs Nerv Syst* 31: 2325-2331. [Crossref]
14. Kato S, Debaud C, Zeller RD (2017) Three-dimensional EOS Analysis of Apical Vertebral Rotation in Adolescent Idiopathic Scoliosis. *J Pediatr Orthop* 37: e543-e547. [Crossref]
15. Fu G, Kawakami N, Goto M, Tsuji T, Ohara T et al. (2009) Comparison of vertebral rotation corrected by different techniques and anchors in surgical treatment of adolescent thoracic idiopathic scoliosis. *J Spinal Disord Tech* 22: 182-189. [Crossref]
16. Delikaris A, Wang X, Boyer L, Larson AN, Ledonio CGT et al. (2018) Implant Density at the Apex Is More Important Than Overall Implant Density for 3D Correction in Thoracic Adolescent Idiopathic Scoliosis Using Rod Derotation and En Bloc Vertebral Derotation Technique. *Spine* 43: E639-E647. [Crossref]
17. Bharucha NJ, Lonner BS, Auerbach JD, Kean KE, Trobisch PD (2013) Low-density versus high-density thoracic pedicle screw constructs in adolescent idiopathic scoliosis: do more screws lead to a better outcome? *Spine J* 13: 375-381. [Crossref]
18. Larson AN, Polly DW, Diamond B, Ledonio C, Richards BS et al. (2014) Does higher anchor density result in increased curve correction and improved clinical outcomes in adolescent idiopathic scoliosis? *Spine* 39: 571-578. [Crossref]
19. Shen M, Jiang H, Luo M, Wang W, Li N et al. (2017) Comparison of low density and high density pedicle screw instrumentation in Lenke 1 adolescent idiopathic scoliosis. *BMC Musculoskelet Disord* 18: 336. [Crossref]
20. Yeh YC, Niu CC, Chen LH, Chen WJ, Lai PL (2019) The correlations between the anchor density and the curve correction of adolescent idiopathic scoliosis surgery. *BMC Musculoskelet Disord* 20: 497. [Crossref]
21. Easwar TR, Hong JY, Yang JH, Suh SW, Modi HN (2011) Does lateral vertebral translation correspond to Cobb angle and relate in the same way to axial vertebral rotation and rib hump index? A radiographic analysis on idiopathic scoliosis. *Eur Spine J* 20: 1095-1105. [Crossref]
22. Duval Beaupère G, Schmidt C, Cosson P (1992) A Barycentremetric study of the sagittal shape of spine and pelvis: the conditions required for an economic standing position. *Ann Biomed Eng* 20: 451-462. [Crossref]
23. Vialle R, Levassor N, Rillardon L, Templier A, Skalli W et al. (2005) Radiographic analysis of the sagittal alignment and balance of the spine in asymptomatic subjects. *J Bone Joint Surg Am* 87: 260-267. [Crossref]
24. Lenke LG, Betz RR, Harms J, Bridwell KH, Clements DH et al. (2001) Adolescent idiopathic scoliosis: a new classification to determine extent of spinal arthrodesis. *J Bone Joint Surg Am* 83: 1169-1181. [Crossref]
25. Schwab F, Ungar B, Blondel B, Buchowski J, Coe J et al. (2012) Scoliosis Research Society-Schwab adult spinal deformity classification: a validation study. *Spine* 37: 1077-1082. [Crossref]